

# ADAPTIVE MOVING GRID METHODS FOR PARTIAL DIFFERENTIAL EQUATIONS

(a series of lectures in Beijing, 2005)

Paul A. Zegeling

June 20, 2005

## 1 Introduction

Traditional numerical techniques to solve time-dependent partial differential equations (PDEs) integrate on a uniform spatial grid that is kept fixed on the entire time interval. If the solutions have regions of high spatial activity, a standard fixed-grid technique is computationally inefficient, since to afford an accurate numerical approximation, it should contain, in general, a very large number of grid points. The grid on which the PDE is discretized then needs to be locally refined. Moreover, if the regions of high spatial activity are moving in time, like for steep moving fronts in reaction-diffusion or hyperbolic equations, then techniques are needed that also adapt (move) the grid in time.

In the realm of adaptive techniques for time-dependent PDEs we can, roughly spoken, distinguish between two classes of methods.

The first class, denoted by the term *h*-refinement, consists of the so-called static-regridding methods. For these methods, the grid is adapted only at discrete time levels. The main advantage of this type of techniques is their conceptual simplicity and robustness, in the sense that they permit the tracking of a varying number of wave fronts. A drawback, however, is that interpolation must be used to transfer numerical quantities from the old grid to new grids. Also, numerical dispersion, appearing, for instance, when hyperbolic PDEs are numerically approximated, is not fully annihilated with *h*-refinement. Another disadvantage of static-regridding is the fact that it does not produce ‘smoothing’ in the time direction, with the consequence

that the time-stepping accuracy therefore will demand small time steps. Examples of this type of methods can be found in Arney et al [4], Berger et al [8], Trompert et al [43].

The second class of methods, denoted by the term  $r$ -refinement (*re*-distribute or *re*-locate), have the special feature to move the spatial grid continuously and automatically in the space-time domain while the discretization of the PDE and the moving-grid procedure are intrinsically coupled. Moving-grid techniques use a fixed number of grid points, without need of interpolation and let the grid points dynamically move with the underlying feature of the PDE (wave, pulse, front, ...). Examples of  $r$ -refinement based methods can be found in Hawken et al [23], Thompson [42], Zegeling [46] and later on in this manuscript. Since the number of grid points is held fixed throughout the course of computation, problems could arise if several steep fronts would act in different regions of the spatial domain. For example, the grid is following one wave front, while a second front arises somewhere else. No ‘new’ grid is created for the new wave front, but rather the ‘old’ one has to adjust itself abruptly to cope with the newly-developed front. Another difficulty is of a topological nature: usually referred to as ‘grid-distortion’ or ‘mesh-tangling’. Especially for higher dimensions this may cause problems, since the accuracy of the numerical approximation of the derivatives depends highly on the grid. Therefore, moving-grid techniques often need additional regularization terms to prevent this from happening or to at least slow down the grid degeneration process. Another possibility is to combine static-regridding with moving grid techniques, as is done in  $h - r$ -refinement methods, see e.g. Arney et al [5] or Petzold [37].

During the last two decades moving grid techniques have been shown to be very useful for solving parabolic and hyperbolic partial differential equations involving fine scale structures such as steep moving moving fronts, emerging steep layers, pulses and shocks. Using  $r$ -refinement for these types of PDEs can save up to several factors in terms of numbers of spatial grid points, if the mesh is moved properly, i.e. without distortion and well-adapted to the underlying PDE solution. For a typical one-dimensional situation, Figure 1 displays the computational efficiency of moving grids compared to fixed uniform grids, i.e. the relation between computational effort (measured in cpu seconds) and the error in the numerical solution (measured as the  $L_2$ -error). In higher space dimensions an ever higher computational efficiency can be measured.

In one space dimension moving-grid methods have been applied successfully to many different types of PDE systems (see e.g. Carlson et al [14], Zegeling et al [47, 46]). In two space dimensions, however, application of

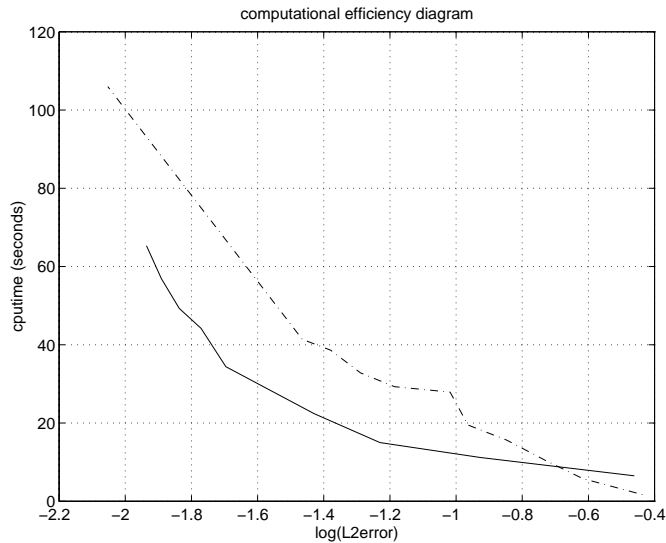


Figure 1: Computational effort as a function of the  $L_2$ -error: fixed (dashed) vs. moving grid (solid).

moving-grid methods is far less trivial than in 1D. For instance, there are many possibilities to treat the one-dimensional boundary and to discretize the spatial domain, each having their own difficulties for specific PDEs. Furthermore, in 2D the chances for grid distortion to occur are much greater due to the extra degree of freedom (see Zegeling et al [48]). In the following sections several moving grid techniques for time-dependent PDEs are discussed. It should be noted, that, in many cases, the method of lines is used, i.e. first the PDE is discretized in the spatial direction yielding a large (stiff) system of initial value ODEs. Then, time-integration of this ODE system, arising from semi-discretizing the PDEs in the discussed examples, is performed by using the integrator Petzold [36].

## 2 Basic Principles

Before examining some moving-grid techniques, it is necessary to prepare a time-dependent PDE for the grid movement. This can be done by defining a coordinate transformation from the physical space (a non-uniform grid for the original PDE) to the computational space, where a uniform grid is used.

## 2.1 Transformation of variables

Underlying all moving grid methods is a transformation between grids. Let, e.g. in one space dimension, a general time-dependent transformation be given by  $x = x(\xi, \theta)$ ,  $t = \theta$ , which carries points from the uniform  $\xi$ -space into corresponding points in non-uniform  $x$ -space. As an example, such a transformation could be given by

$$x(\xi, \theta) = e^{-\theta}\xi + (1 - e^{-\theta})\frac{1}{\nu} \ln(1 + (e^\nu - 1)\xi), \quad \text{for } \theta \in [0, 10], \xi \in [0, 1], \nu > 0. \quad (1)$$

In Figure 2 this transformation is displayed for  $\nu = 10$ . This transformation and its grid (uniform in  $\xi$  direction and therefore stretched in  $x$  direction) can be used to follow a PDE solution that ends in a steep boundary layer at  $x = 1$  and  $t = \theta \gg 1$ . For example, we could take  $u(x, t) = (1 - e^{-t})\frac{e^{\lambda x} - 1}{e^{\lambda} - 1}$  as a possible PDE solution, with  $\lambda = 100$  and  $\theta = 10$ . Starting with a uniform grid at  $t = \theta = 0$ , i.e.  $x(\xi, 0) = \xi$ , a moving grid is obtained as shown in the two right plots of Figure 2.

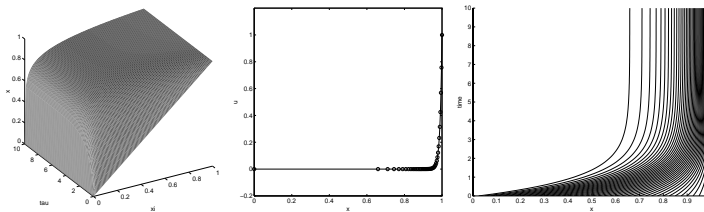


Figure 2: Transformation (1) (left), solution at  $\theta = 10$  (middle), and grid history (right).

Consider now the time-dependent PDE in two space dimensions (the one-dimensional case is obtained by freezing the second space direction)

$$\frac{\partial u}{\partial t} = \delta \Delta u - \beta \cdot \nabla u + S(u, \underline{x}, t) \equiv \mathcal{L}(u), \quad (2)$$

for  $\underline{x} \in \Omega \subset \mathbb{R}^2$ ,  $t > 0$  with given boundary conditions on  $\partial\Omega$  and initial condition for  $t = 0$ . The PDE operator  $\mathcal{L}$  contains spatial derivatives of  $u$ . We seek for a solution  $u(\underline{x}, t)$  with  $\underline{x} \in \Omega \equiv [0, 1]^2$  and  $t \in [0, T]$ . For general domains  $\Omega$ , an extra transformation will be needed between the parametric and the physical domain.

For the two-dimensional PDE (2) we can define a transformation  $x = x(\xi, \eta, \theta)$ ,  $y = y(\xi, \eta, \theta)$ ,  $t = \theta$ . Then applying the chain rule for differentiation we get

$$\frac{\partial u}{\partial \theta} = \frac{\partial u}{\partial t} + \frac{\partial u}{\partial x} \frac{\partial x}{\partial \theta} + \frac{\partial u}{\partial y} \frac{\partial y}{\partial \theta}, \quad (3)$$

where

$$\frac{\partial u}{\partial x} = 0 + \frac{\partial u}{\partial \xi} \frac{\partial \xi}{\partial x} + \frac{\partial u}{\partial \eta} \frac{\partial \eta}{\partial x}, \quad \text{and} \quad \frac{\partial u}{\partial y} = 0 + \frac{\partial u}{\partial \xi} \frac{\partial \xi}{\partial y} + \frac{\partial u}{\partial \eta} \frac{\partial \eta}{\partial y}.$$

Substituting these equations in PDE (2), the transformed PDE reads

$$u_\theta + \frac{1}{\mathcal{J}} [u_\xi (y_\theta x_\eta - x_\theta y_\eta) + u_\eta (x_\theta y_\xi - y_\theta x_\xi) - u_\xi (-\beta_1 y_\eta + \beta_2 x_\eta) - u_\eta (\beta_1 y_\xi - \beta_2 x_\xi)] = \quad (4)$$

$$\frac{\delta}{\mathcal{J}} \left[ \left( \frac{x_\eta^2 + y_\eta^2}{\mathcal{J}} u_\xi \right)_\xi - \left( \frac{y_\xi y_\eta + x_\xi x_\eta}{\mathcal{J}} u_\eta \right)_\xi - \left( \frac{y_\xi y_\eta + x_\xi x_\eta}{\mathcal{J}} u_\xi \right)_\eta + \left( \frac{x_\xi^2 + y_\xi^2}{\mathcal{J}} u_\eta \right)_\eta \right] + S(u, x, y, \theta),$$

where  $\mathcal{J} = x_\xi y_\eta - x_\eta y_\xi$  is the Jacobian of the transformation.

In one space dimension this may be written as the Lagrangian form of the PDE:

$$\dot{u} - u_x \dot{x} = \mathcal{L}(u),$$

where the dot stands for  $\frac{\partial}{\partial \theta}$ , and  $u_x$  for  $u_\xi / x_\xi = u_\xi / \mathcal{J}$ . Semi-discretizing (4) in the spatial direction, we get a system of ordinary differential equations (ODEs). To complete the system, additional equations (ODEs or PDEs) for the grid movement  $x_\theta$  and  $y_\theta$  are required. This will be presented in the following sections.

## 2.2 The Method of Characteristics (MoC)

One of the ‘simplest’ choices for letting the grid move and implicitly defining the transformation is to make use of the characteristic equations of the PDE. This is, of course, only feasible for a small class of hyperbolic systems. If we consider the transport equation  $\frac{\partial u}{\partial t} = -\beta \nabla u + \gamma$ , then MoC (see Courant et al [16]) leads to  $\frac{\partial}{\partial \theta} \underline{x} = \beta$  and  $\frac{\partial u}{\partial \theta} = \gamma$ . Note that, if these equations are combined then we obtain the equivalent equation  $\frac{\partial u}{\partial \theta} - \nabla u \cdot \frac{\partial}{\partial \theta} \underline{x} = \beta \nabla u + \gamma$ , which is the original PDE but now in the computational domain.

Using moving-grid equations based on MoC, we can produce extremely accurate numerical solutions for this type of PDEs. Note that, although the pointwise error is extremely low, the moving peak is very poorly resolved (with only 5 grid points). Or, in terms of the coordinate transformation:  $\partial x / \partial \xi = 1$ . This is shown for  $\beta = 1$ ,  $\gamma = 0$  in a 1D situation with 21

grid points in Figure 3. In the case of  $x := \xi$ ,  $\forall \theta \geq 0$  (a non-moving uniform grid) numerical solutions would have produced unwanted oscillations and/or severe unnatural damping. The MoC approach is not well-suited for general hyperbolic PDEs, however: a standard counterexample is given by the choice  $\beta = u$ ,  $\gamma = 0$  (Burgers' equation), for which the PDE characteristics collide at some point of time and therefore must give colliding grid points. In higher space dimensions this situation will only deteriorate. This feature is also shown in Figure 3 (right plot) for the 2D case, where  $\beta = \pi(y - \frac{1}{2}, \frac{1}{2} - x)^T$ . The characteristic trajectories are now given by circles around  $(x, y) = (\frac{1}{2}, \frac{1}{2})$  on which the time-variable  $\theta$  varies. Using MoC to move the grid would produce a twisted and distorted grid. It should therefore be clear that, in general, MoC is not the way to let the grid move, at least without additional re-meshing.

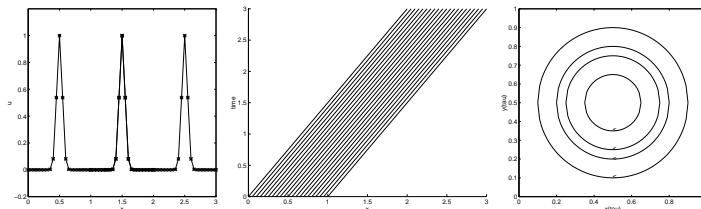


Figure 3: Using the method of characteristics in 1D (left and middle); right: example of characteristics in 2D that will certainly twist the underlying grid.

### 2.3 Equidistribution

One of the most widely-spread concepts to adapt and move a grid in one space dimension is given by the so-called equidistribution principle; cf. De Boor [11], Ren et al [39]. In this case the (inverse) coordinate transformation is explicitly given as

$$\xi(x, t) = \int_0^x M(\tilde{x}, t) d\tilde{x} / \int_0^1 M(\tilde{x}, t) d\tilde{x},$$

which is equivalent to

$$\int_0^{x(\xi, t)} M(\tilde{x}, t) d\tilde{x} = \xi \int_0^1 M(\tilde{x}, t) d\tilde{x}, \quad (5)$$

where  $M > 0$  is a so-called monitor or weight function, usually depending on first and second-order spatial derivatives of the PDE solution. If we select

$N - 1$  time-dependent grid points defining the spatial grid:

$$X : 0 = X_0 < \dots < X_i(t) < X_{i+1}(t) < \dots < X_N = 1, \quad t > 0,$$

and using a uniform grid in the  $\xi$ -direction ( $\xi_i = i/N$ ) equation (5) can be ‘discretized’ as

$$\int_{x(\xi_{i-1}, t)}^{x(\xi_i, t)} M d\tilde{x} = \frac{1}{N} \int_0^1 M d\tilde{x}, \quad \text{for } i = 1, \dots, N, \quad (6)$$

with  $x(\xi_i, t) = X_i(t)$ . We can also differentiate (5) twice with respect to  $\xi$  to obtain the PDE

$$\frac{\partial}{\partial \xi} \left( \frac{\partial x}{\partial \xi} M \right) = 0. \quad (7)$$

Using the midpoint rule for evaluating the integrals in (6), we obtain yet another formula that describes equidistribution:

$$\Delta X_{i-1} M_{i-1} = \Delta X_i M_i, \quad 1 \leq i \leq N - 1, \quad (8)$$

where  $M_i \equiv M|_{x=X_{i+\frac{1}{2}}}$  and  $\Delta X_i = X_{i+1} - X_i$ . This discretized form, which is equivalent to  $\Delta X_i M_i = \text{constant}$ , states that the grid should be moved to places where the weight function  $M$  dominates. More precisely, the grid cells  $\Delta X_i$  should be small where  $M_i$  is large, and  $\Delta X_i$  should be large where  $M_i$  is small, respectively, since the product of both quantities is constant. In other words, referring to (6): the grid points are re-distributed by ‘distributing the weight function  $M$  equally over all subintervals’. It is also noted that PDE (7) can be obtained by minimizing the energy integral  $I = \int_0^1 M x_\xi^2 d\xi$ , which can be taken to represent the energy of a system of springs with spring constants  $M$ , cf. Thompson [42]. The grid point distribution then would represent the equilibrium state of such a spring system. As an example in 1D the Lagrangian PDE (4) could be combined with the moving grid PDE (cf. (7))  $\frac{\partial x}{\partial \theta} = \frac{\partial}{\partial \xi} \left( \frac{\partial x}{\partial \xi} M \right)$ , where  $\theta$  is now playing the role of an artificial time-variable. In Figure (4) (left and middle) the grid and solution (- -) are shown for this case ( $N = 21$ ) with the arc-length monitor  $M = \sqrt{1 + u_x^2}$ . The exact ‘solution’  $u = \sin^{100}(\pi x)$  is being used. It is clearly seen that the first derivative of  $u$  is over-emphasized. Some smoothing is therefore needed to provide more regularly distributed grid ratios. This will be worked out in the next subsection.

In two space dimensions there is no straightforward extension of this principle, see, however, sections 3.1, 3.3.1 and Baines [7], Dwyer et al [21], Huang et al [27] for some ways to define equidistribution-like methods in higher dimensions.

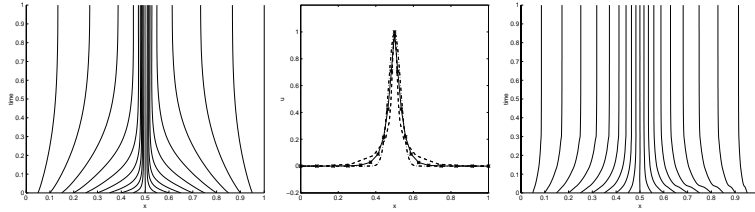


Figure 4: Left: grid for the equidistribution equation (8); middle: solution  $u$  (with - -), the exact solution (with -), solution for  $\sigma = 2$  (with -\*); right: smoothed grid.

### 3 More Advanced Techniques

#### 3.1 Moving Finite Differences (MFD)

Starting from the equidistribution principle described by (8), it is easy to derive a moving grid technique with a ‘smooth’ behaviour in space and time. For this purpose we introduce the point-concentration values  $n_i \equiv (\Delta X_i)^{-1}$ ,  $0 \leq i \leq N$ , and the relation (8) is rewritten as

$$n_{i-1}/M_{i-1} = n_i/M_i, \quad 1 \leq i \leq N - 1. \quad (9)$$

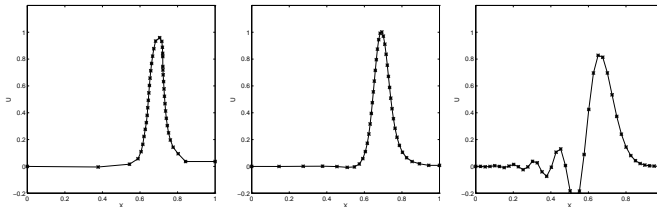


Figure 5: Numerical solutions with too little spatial smoothing (left;  $\sigma = 0.2$ ), with ‘standard’ spatial smoothing (middle;  $\sigma = 2$ ), and with too much smoothing (right;  $\sigma = 100$ ).

When using equation (8) (or (9)) there is little control over the grid movement. For example, it can happen that the grid distance  $\Delta X_i$  varies extremely rapidly over  $X$  (see Figure (4); left plot) or that for evolving time the trajectories  $X_i(t)$  tend to oscillate. Too large a variation in  $\Delta X_i$  may be detrimental to spatial accuracy and temporal grid oscillations are likely to hinder the numerical time-stepping since the grid trajectories are computed

automatically by numerical integration. Therefore, two grid-smoothing procedures are added: one for generating a spatially smooth grid and the other for avoiding temporal grid oscillations. This involves a modification of system (9). Instead of (9) the grid motion is now given by the system of ordinary differential equations

$$(\tilde{n}_{i-1} + \tau_s \frac{d}{dt} \tilde{n}_{i-1})/M_{i-1} = (\tilde{n}_i + \tau_s \frac{d}{dt} \tilde{n}_i)/M_i, \quad t > 0, \quad 1 \leq i \leq N, \quad (10)$$

where  $\tilde{n}_i = n_i - \sigma(\sigma + 1)(n_{i+1} - 2n_i + n_{i-1})$  with  $\sigma \geq 0$ . The parameter  $\sigma$  is connected with the spatial grid-smoothing. It can be proved, Verwer et al [44], that the moving grid defined by (10) satisfies

$$\frac{\sigma}{\sigma + 1} \leq \frac{\Delta X_{i+1}(t)}{\Delta X_i(t)} \leq \frac{\sigma + 1}{\sigma} \quad \forall i, \quad t \geq 0 \quad (11)$$

showing that we have control over the variation in  $\Delta X_i$  for all points of time. The parameter  $\tau_s \geq 0$  in (10) is connected with the temporal grid-smoothing and serves to act as a delay factor for the grid movement. The introduction of the temporal derivative of the grid  $X$  (via  $\frac{d}{dt} \tilde{n}_i$  in (10)) forces the grid to adjust over a time interval of length  $\tau_s$  from old to new monitor values, which provides a tool for suppressing grid oscillations in time.

Combining system (10) with the 1D semi-discrete form of (4) gives the stiff ODE system

$$\mathcal{A}_{mfd}(\eta_1, \tau_s) \dot{\eta}_1 = G_{mfd}(\eta_1), \quad (12)$$

with  $\eta_1 \equiv (\dots, U_i, X_i, \dots)^T$ . A well-known choice for the monitor is  $M_i = \sqrt{1 + \alpha \frac{(U_{i+1} - U_{i-1})^2}{(X_{i+1} - X_{i-1})^2}}$ , where  $\alpha \geq 0$  is an adaptivity parameter. For  $\alpha = 1$  we have the arc-length monitor (see 2.3) which places grid points along uniform arc-length intervals. For  $\alpha = 0$  the monitor function  $M = 1$ , and then (10) yields a uniform grid, while for  $\alpha > 1$  the adaptivity increases as the first spatial derivative  $u_x$  is more emphasized. A ‘standard’ choice for the three method parameters is:  $\alpha = 1$ ,  $\sigma = 2$ ,  $\tau_s = 10^{-3}$  (see Furzeland et al [22]). In Figure 5 the effect of spatial smoothing is depicted at  $t = \frac{1}{2}$  when (10) is applied to the scalar advection equation  $\frac{\partial u}{\partial t} + \frac{\partial u}{\partial x} = 0$  with the analytical solution  $u^*(x, t) = \sin^{50}(\pi(x - t + \frac{3}{10}))$ . Note that too little or too much smoothing may give rise to irregular grids (left) and oscillatory solutions (right), whereas ‘standard’ smoothing produces regular grid positioning and solution behaviour (middle).

It is interesting to note that Huang et al [24] have derived a continuous formulation for (10) in terms of the transformation variables  $\xi$  and  $\theta$ . The

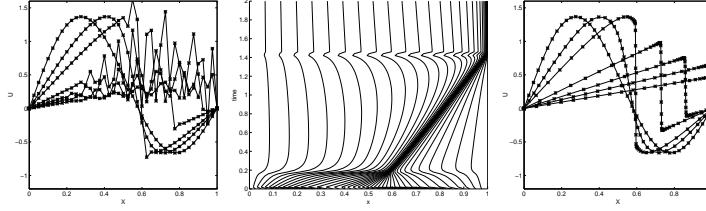


Figure 6: Numerical solutions of the 1D Burgers equation (14) with finite differences; left: uniform grid solutions; middle and right: the grid evolution and solution with moving grids.

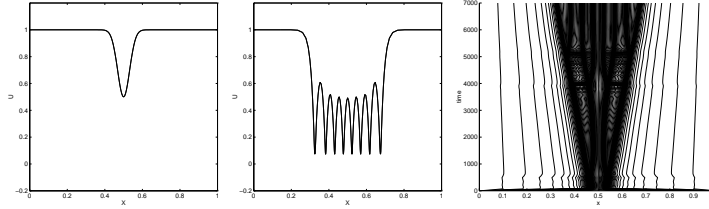


Figure 7: Moving finite differences for the 1D reaction-diffusion system (15) at  $t = 0$  (left),  $t = 7000$  (middle), and the moving grid (right).

ODEs in (10) are then semi-discretized versions of the PDE

$$\frac{\partial}{\partial \xi} \left[ \frac{\tilde{n} + \tau_s \dot{\tilde{n}}}{M} \right] = 0, \quad (13)$$

where  $n \equiv 1/\frac{\partial x}{\partial \xi}$  (the inverse of the Jacobian of the transformation),  $\tilde{n} \equiv (I - (\Delta \xi)^2 \sigma(\sigma + 1) \frac{\partial^2}{\partial \xi^2})n$  and  $M = \sqrt{1 + \alpha u_x^2}$ .

Figure (6) shows numerical results for this moving-grid method ( $N = 41$ ) when applied to Burgers' equation with spatial operator

$$\mathcal{L}(u) = \delta \frac{\partial^2 u}{\partial x^2} - u \frac{\partial u}{\partial x}, \quad (14)$$

and  $\delta = 5 \cdot 10^{-4}$ ,  $u|_{t=0} = \frac{1}{2} \sin(\pi x) + \sin(2\pi x)$ ,  $u|_{\partial \Omega} = 0$ . In the left plot the well-known 'wiggles' are seen for the non-moving grid case. The moving grid ((middle and right plot) follows the sharpening of the solution and moving front satisfactorily.

Figure (7) shows further numerical results for this method when applied to

a system of reaction-diffusion equations with

$$\mathcal{L}_1(u, v) = \Delta u - uv^2 + A(1 - u), \quad (15)$$

$$\mathcal{L}_2(u, v) = 10^{-2}\Delta v + uv^2 - Bv,$$

and constants  $A$  and  $B$ , an initial steep pulse in the middle of the domain and Dirichlet boundary conditions (see Doelman et al [20] for more details).

As stated before, in two dimensions no proper mathematical definition for equidistribution exists. However, it is possible to define one-dimensional equidistribution (with smoothing) along co-ordinate lines in 2D. For example (see also Zegeling [50]), one can define the moving grid by

$$\begin{aligned} \frac{\partial}{\partial \xi} \left[ \frac{\tilde{n} + \tau_s \dot{\tilde{n}}}{M_{(x)}} \right] &= 0, \quad \text{with } n \equiv 1/x_\xi, \\ \frac{\partial}{\partial \eta} \left[ \frac{\tilde{m} + \tau_s \dot{\tilde{m}}}{M_{(y)}} \right] &= 0, \quad \text{with } m \equiv 1/y_\eta, \end{aligned} \quad (16)$$

where

$$M_{(x)} \equiv \sqrt{1 + \alpha u_x^2}, \quad M_{(y)} \equiv \sqrt{1 + \alpha u_y^2},$$

and

$$\tilde{n} \equiv (I - (\Delta \xi)^2 \sigma(\sigma + 1) \frac{\partial^2}{\partial \xi^2})n, \quad \tilde{m} \equiv (I - (\Delta \eta)^2 \sigma(\sigma + 1) \frac{\partial^2}{\partial \eta^2})m.$$

At the boundary Neumann conditions for the grid are imposed:  $\frac{\partial n}{\partial \xi}|_{x=0} = \frac{\partial n}{\partial \xi}|_{x=1} = \frac{\partial m}{\partial \eta}|_{y=0} = \frac{\partial m}{\partial \eta}|_{y=1} = 0$ . Semi-discretizing the PDEs in (16) in the spatial direction with central differences and defining  $\eta_2 \equiv (\dots, U_i, X_i, Y_i, \dots)^T$  it can be written as:

$$\mathcal{A}_{mfd}(\eta_2, \tau_s) \dot{\eta}_2 = G_{mfd}(\eta_2). \quad (17)$$

Figure 8 shows solutions and grids for the hyperbolic PDE with

$$\mathcal{L}(u) = \pi(y - \frac{1}{2}) \frac{\partial u}{\partial x} + \pi(\frac{1}{2} - x) \frac{\partial u}{\partial y}, \quad (18)$$

for  $u|_{t=0} = e^{-100((x-\frac{1}{2})^2 + (y-\frac{13}{20})^2)}$ ,  $u|_{\partial\Omega} = 0$  and two points of time:  $t = \frac{1}{2}$  and  $t = 1$ . The solution of the PDE is a pulse that rotates without change of shape around the center of the domain. This is a difficult test problem for standard numerical techniques. In the moving grid case almost no numerical

diffusion or oscillations appear, in contrast with the non-moving situation (see also Table 1). A second example is a model used in hydrology. It is an advection-dispersion equation with a moving front that starts from the left boundary and moves into the centre of the domain. A practical situation is described by the spatial PDE operator

$$\mathcal{L}(u) = 10^{-3} \frac{\partial^2 u}{\partial x^2} + 10^{-2} \frac{\partial^2 u}{\partial y^2} - \frac{\partial u}{\partial x}, \quad (19)$$

with initial condition  $u|_{t=0} = \frac{1}{4}(1 + \tanh(50(\frac{1}{32} - (y - \frac{1}{2})^2)))(1 + \tanh(50(\frac{1}{32} - x^2)))$ , and Neumann boundary conditions, except for that part of the boundary  $x = 0$  where the solution is initially maximal (there a Dirichlet condition is imposed). In Figure 9 the grids, that are nicely located near the steep front, are displayed for  $t = 0.06$  and  $t = 0.48$ .

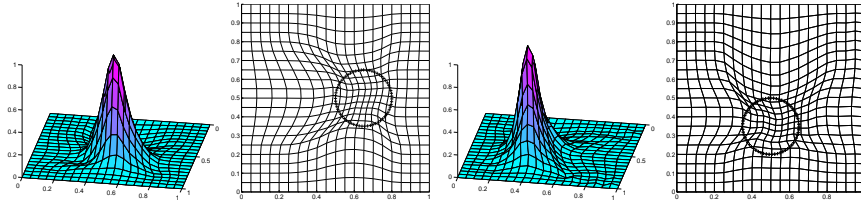


Figure 8: Moving finite difference results for the 2D advection PDE (18). With + the position of the pulse is depicted.

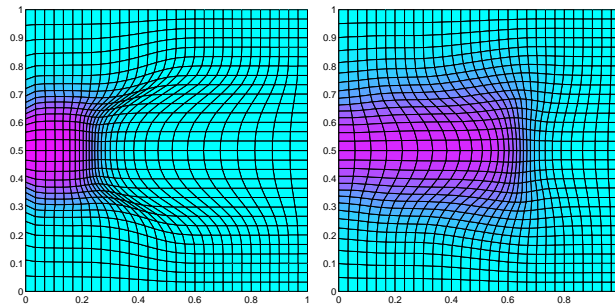


Figure 9: Moving finite difference results for the 2D advection-dispersion PDE (19) at  $t = 0.06$  (left) and  $t = 0.48$  (right).

### 3.2 Moving Finite Elements (MFE)

A two-dimensional moving grid technique (MFE) based on the minimization of the PDE residual is obtained by approximating the PDE solution  $u$  with piecewise-linear finite element basis functions (see Baines [6], Miller et al [34, 35], Zegeling [49]). There are several ways to describe this method. Here, we follow the concept of the transformation between the physical and computational domain:

$$u \approx U = \sum_{j \in J} U_j(\theta) \alpha_j(\xi, \eta), \quad x \approx X = \sum_{j \in J} X_j(\theta) \alpha_j(\xi, \eta), \quad y \approx Y = \sum_{j \in J} Y_j(\theta) \alpha_j(\xi, \eta), \quad (20)$$

where  $\alpha_j$  are the standard ‘hat’ functions on 2D having a limited support and  $J$  stands for the index set of the grid points. Substituting (20) into the time-dependent PDE model gives, in general, a non-zero PDE residual  $U_t - \mathcal{L}(U)$ . To obtain equations for the grid movement, a minimization procedure (‘least squares’) is applied with respect to the, yet unknown, variables  $\dot{U}_i, \dot{X}_i, \dot{Y}_i$  of the following quantity

$$\int_{\Omega_{\xi, \eta}} (\dot{U} - U_x \dot{X} - U_y \dot{Y} - \mathcal{L}(U))^2 \mathcal{J} \, d\xi d\eta \quad \forall i \in J. \quad (21)$$

Here  $\mathcal{J}$  denotes the Jacobian of the transformation. After re-writing (21) in the physical co-ordinates, we obtain the system

$$\begin{aligned} \int_{\Omega} (U_t - \mathcal{L}(U)) \alpha_i \, dx dy &= 0, \quad \forall i \in J, \\ \int_{\Omega} (U_t - \mathcal{L}(U)) U_x \alpha_i \, dx dy &= 0 \quad \forall i \in J, \\ \int_{\Omega} (U_t - \mathcal{L}(U)) U_y \alpha_i \, dx dy &= 0 \quad \forall i \in J. \end{aligned} \quad (22)$$

Working out the innerproducts and adding small regularization terms  $P_{1,2}$  and  $Q_{1,2}$  to keep the finite-element parametrization non-degenerate, yields for  $i \in J$ :

$$\begin{aligned} \sum_{l \in J} \langle \alpha_i, \alpha_l \rangle \dot{U}_l + \langle \alpha_i, \beta_l \rangle \dot{X}_l + \langle \alpha_i, \gamma_l \rangle \dot{Y}_l &= \langle \alpha_i, \mathcal{L}_i(U) \rangle \\ \sum_{l \in J} \langle \beta_i, \alpha_l \rangle \dot{U}_l + \langle \beta_i, \beta_l \rangle \dot{X}_l + \langle \beta_i, \gamma_l \rangle \dot{Y}_l + P_1(\epsilon_1^2) &= \langle \beta_i, \mathcal{L}_i(U) \rangle + Q_1(\epsilon_2^2) \\ \sum_{l \in J} \langle \gamma_i, \alpha_l \rangle \dot{U}_l + \langle \gamma_i, \beta_l \rangle \dot{X}_l + \langle \gamma_i, \gamma_l \rangle \dot{Y}_l + P_2(\epsilon_1^2) &= \langle \gamma_i, \mathcal{L}_i(U) \rangle + Q_2(\epsilon_2^2), \end{aligned}$$

where  $\beta_i = -U_x \alpha_i$ ,  $\gamma_i = -U_y \alpha_i$  and  $\langle \bullet, \bullet \rangle$  is the standard  $L_2$ -innerproduct. Using  $\eta_2 = (\dots, U_i, X_i, Y_i, \dots)^T$  as before this can be re-written as:

$$\mathcal{A}_{mfe}(\eta_2, \epsilon_1^2) \eta_2 = G_{mfe}(\eta_2, \epsilon_2^2). \quad (23)$$

The small parameters  $\epsilon_1^2$  and  $\epsilon_2^2$  serve to keep the extended mass-matrix  $\mathcal{A}_{mfe}$  and the right-handside  $G_{mfe}$  non-singular, respectively. It is worthwhile to note that the previous derivation can easily be done in higher space dimensions as well.

The more sophisticated GWMFE (see Carlson et al[14, 15]) uses an additional gradient-weighting term in the innerproducts of the form  $\langle w(\nabla U) \bullet, \bullet \rangle$ . However, in general, the results shown below hold, for the greater part, also for GWMFE, possibly with some minor modifications.

Some properties of the moving grid for MFE:

Consider now the PDE (2) in one or two space dimensions. In one space dimension it can be shown, Zegeling et al [48], that for  $\#J \rightarrow \infty$  and  $\epsilon_1^2 = \epsilon_2^2 = 0$  the grid moves as a perturbed method of characteristics:

$$\frac{\partial x}{\partial \theta} = \beta + \delta \left( 2 \frac{u_{xxx}}{u_{xx}} - 3 \frac{\xi_{xx}}{\xi_x} \right), \quad (24)$$

where  $\xi$  is the spatial co-ordinate in the computational domain. Numerical solutions of (23) for Burgers' equation (14), clearly indicating property (24), are given in Figure 10. From equation (24) it can be derived that for steady-state situations ( $\frac{\partial x}{\partial \theta} = \frac{\partial u}{\partial t} = 0$ ) an equidistribution-like relation holds for the grid:

$$\frac{\partial x}{\partial \xi} |u_{xx}|^{2/3} |u_x|^{1/3} = \text{constant}. \quad (25)$$

In two space dimensions it is known that the grid moves in a similar way:

$$\frac{\partial x}{\partial \theta} = \beta_1 + \delta \phi_1, \quad (26)$$

$$\frac{\partial y}{\partial \theta} = \beta_2 + \delta \phi_2.$$

However, an explicit formulation for the perturbation functions  $\phi_1$  and  $\phi_2$  has not been derived yet. Numerical experiments suggest that they should depend on first and second-order spatial derivatives. This behaviour 'between' equidistribution (equation (25)) and the method of characteristics (eq. (24)) is illustrated in Figures 11 and 12. In Figure 11 it is concluded that the grid in the method follows the flow of a hyperbolic PDE, whereas for diffusion dominated PDEs the grids concentrate near regions of high

spatial activity (first and second-order derivatives of the solution). Figure 12 confirms this property by letting the diffusion coefficient  $\delta$  decrease from 1 to  $10^{-3}$  for the PDE with

$$\mathcal{L}(u) = \delta \Delta u + (x - \frac{1}{2}) \frac{\partial u}{\partial x} - (y - \frac{1}{2}) \frac{\partial u}{\partial y} + f(x, y, t), \quad (27)$$

and  $u|_{t=0} = 0$ ,  $u|_{\partial\Omega} = 0$ . The source term  $f(x, y, t)$  is defined as

$$f(x, y, t) = u_t^* - \delta \Delta u^* - (x - \frac{1}{2}) \frac{\partial u^*}{\partial x} + (y - \frac{1}{2}) \frac{\partial u^*}{\partial y},$$

such that  $u^*(x, y, t) = \frac{1}{2}(1 - e^{-t})(1 + \tanh(100(\frac{1}{16} - (x - \frac{1}{2})^2 - (y - \frac{1}{2})^2)))$  is the exact solution of the PDE model. This means that in steady-state we always must have the same solution, which is a steep circular ‘hat’ in the middle of the domain (depicted by +’s in the figure). We see that the grid is ‘equidistributed’ for larger values of  $\delta$  and ‘distorted’, following the first derivative terms, for lower values of the diffusion parameter (i.e. perturbed MoC). Another example to show the dependence of MFE on the PDE characteristics is given in Figure 13 and Table 1, where solutions and grids are given for the hyperbolic PDE (18). To stress the equidistribution property of MFE for parabolic PDEs, numerical results for MFE when applied to the 2D version of the reaction-diffusion PDE system (15) are depicted in Figure 14. For this model the grid points are nicely located in areas of high spatial activity, i.e. where first and second-order derivatives dominate.

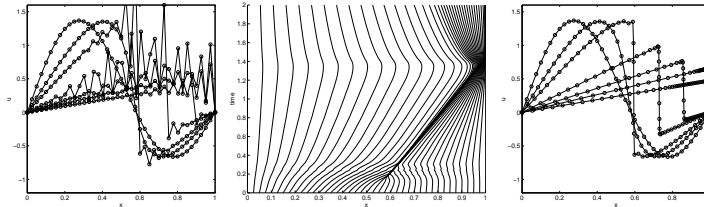


Figure 10: Numerical solutions of the 1D Burgers equation (14) with finite elements; left: (oscillatory) uniform grid solutions; middle and right: the grid evolution and (non-oscillatory) solution with moving grids.

Method	$U_{max}(t = 0.5)$	$U_{min}(t = 0.5)$	$U_{max}(t = 1.0)$	$U_{min}(t = 1.0)$	Grid	Solution
FFE	0.7863	-0.0011	0.6338	-0.0022	uniform	numerically diffused
MFE	1.0027	-0.0040	1.0056	-0.0258	‘distorted’	almost exact
FFD	0.8985	-0.0914	0.7784	-0.1637	uniform	very inaccurate
MFD	0.9430	-0.0106	0.9360	-0.0283	adaptive	rather accurate

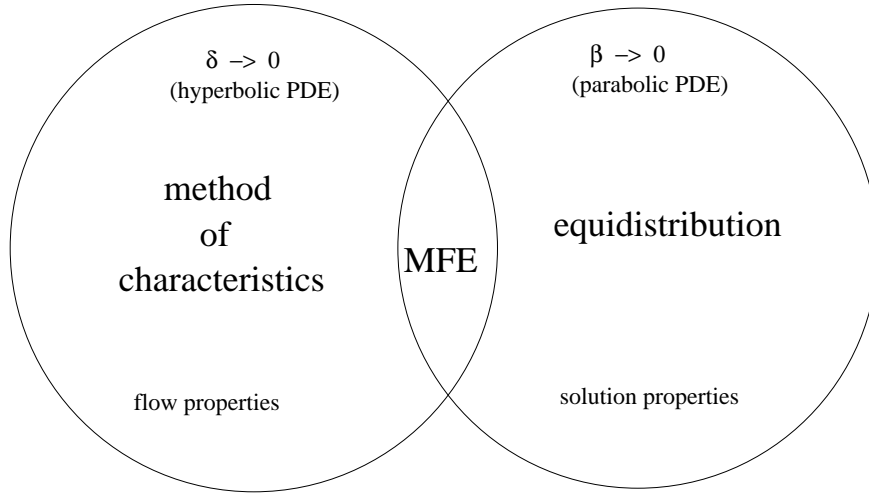


Figure 11: The Moving Finite Element method has a relation both with equidistribution and with MoC.

Table 1. Numerical results for the 2D advection model (18) using MFE, MFD and uniform non-moving grids (FFE and FFD). Maximum and minimum values of the solution should be 1 and 0, respectively.

### 3.3 Related Approaches

#### 3.3.1 The Deformation method

Recently, a new moving grid approach was developed which can be formulated in ‘any’ space dimension. In some sense, it can be seen as an extension of the equidistribution principle to higher dimensions. This approach, also denoted by the ‘deformation method’ which stems from the theory of volume elements of a compact Riemannian manifold, Liao et al [31, 32], was first used for given steep functions by Bochev et al [10], steady-state PDEs by Liao et al [33], and time-dependent PDEs in 1D by Semper et al [40]. To be consistent with the previous sections we will describe the ideas behind the method in two dimensions, although it can be done in a more general context.

The movement of the grid in the deformation method is described by

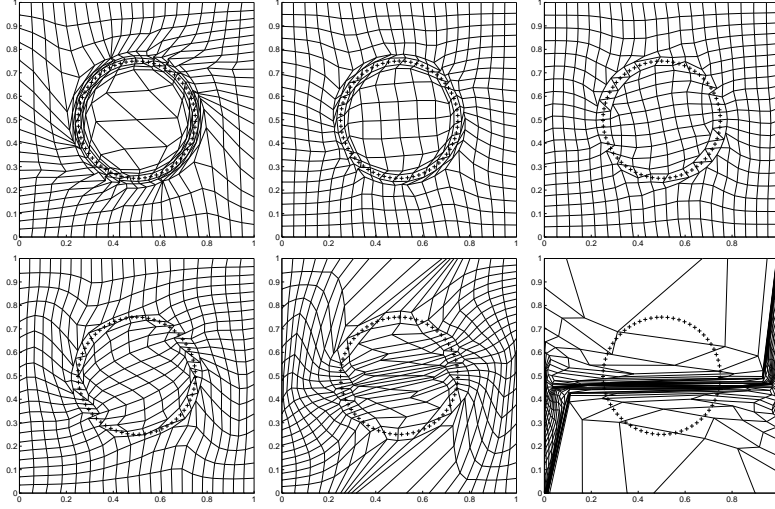


Figure 12: Moving finite element grids for the convection-diffusion PDE (27) for decreasing values of the diffusion coefficient  $\delta$ . With + the position of the steady-state solution is depicted.

the grid PDEs:

$$\frac{\partial x}{\partial \theta} = -v_1/W_l, \quad (28)$$

$$\frac{\partial y}{\partial \theta} = -v_2/W_l,$$

where the vectorfield  $v \equiv (v_1, v_2)^T$  should satisfy

$$\nabla \cdot v = -\frac{\partial W_l}{\partial t}, \quad v|_{\partial\Omega} = 0. \quad (29)$$

Here  $W_l$  is a (scaled) positive weight function, e.g.  $W_l = M_l / \int_{\Omega} M_l d\Omega$ , with (unscaled)  $M_l = 1 + \alpha_l u^2 + \beta_l \|\nabla u\|_2^2$ , such that  $\int_{\Omega} W_l d\Omega = 1$ ,  $\forall t = \theta \geq 0$ . It can be shown ([10]) that from (28) and (29) follows

$$\det(\mathcal{J}) \cdot W_l = 1, \quad \forall t = \theta \geq 0, \quad (30)$$

where  $\mathcal{J}$  is the Jacobian of the transformation as mentioned in Section 2.1.

In one space dimension equation (30) reduces to

$$\frac{\partial x}{\partial \xi} W_l = 1, \quad \forall t = \theta \geq 0, \quad (31)$$

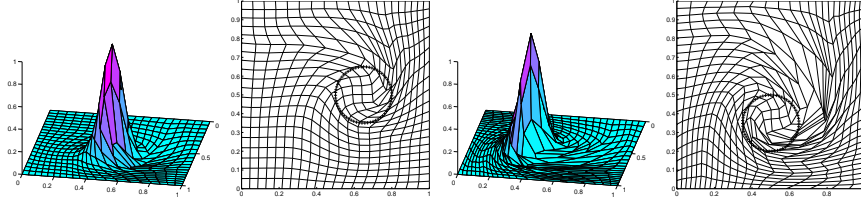


Figure 13: Moving finite element results for the 2D advection PDE (18). With + the position of the pulse is depicted.

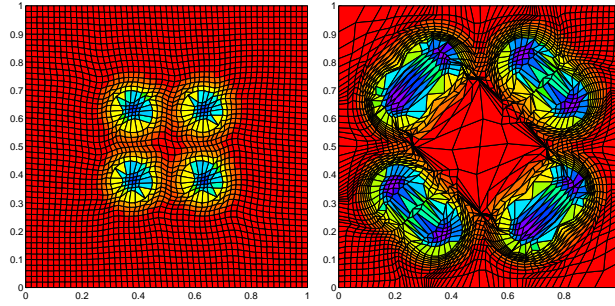


Figure 14: Moving finite element results for the 2D reaction-diffusion system (15) at  $t = 10$  and  $t = 500$ .

giving an equidistribution relation which is an integral of PDE (7) with integration constant equal to 1. A consequence of equation (30) is that the Jacobian of the transformation will always remain non-zero if  $W_l$  is positive. In a discretized form this means that the grid can not distort, since the transformation is ‘held’ non-singular. For the 1D case a straightforward integration of (29) yields

$$v = - \int_0^x \frac{\partial W_l}{\partial t} d\tilde{x}, \quad (32)$$

defining the moving grid equation uniquely. In 2D, however, no unique solution exists for (29), which means that, for example, a least-squares technique has to be used to define the vector field  $v$ . On the other hand, it is possible to construct one solution that satisfies (29) in two space dimensions:

$$v_1 = \frac{1}{2} \left( - \int_0^x \frac{\partial W_l}{\partial t} d\tilde{x} + h(x) \int_0^1 \frac{\partial W_l}{\partial t} d\tilde{x} - h'(y) \int_0^x \int_0^1 \frac{\partial W_l}{\partial t} d\tilde{y} d\tilde{x} \right), \quad (33)$$

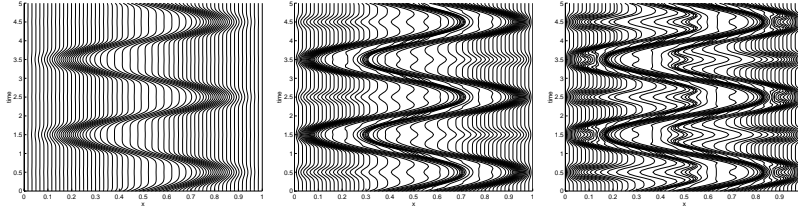


Figure 15: Grids for the deformation method in 1D;  $\alpha_l = 1, \beta_l = \gamma_l = 0$  (left),  $\alpha_l = \gamma_l = 0, \beta_l = 10^{-2}$  (middle) and  $\alpha_l = \beta_l = 0, \gamma_l = 10^{-4}$  (right).

$$v_2 = \frac{1}{2} \left( - \int_0^y \frac{\partial W_l}{\partial t} d\tilde{y} + h(y) \int_0^1 \frac{\partial W_l}{\partial t} d\tilde{y} - h'(x) \int_0^y \int_0^1 \frac{\partial W_l}{\partial t} d\tilde{x} d\tilde{y} \right), \quad (34)$$

where  $h(\zeta) = \frac{1}{2}(1 + \cos(\zeta))$ . In Figure (15) deforming grids are shown for a scalar PDE with  $\mathcal{L}(u) = -\cos(\pi t) \frac{\partial u}{\partial x}$ ,  $u|_{t=0} = \sin^{10}(\pi x)$ ,  $u|_{\partial\Omega} = 0$  and the exact solution  $u^*(x, t) = \sin^{10}(\pi(x - \sin(\pi t)/\pi))$ . The difference in positioning of the grid points can be seen clearly, depending on the choices for the parameters  $\alpha_l$ ,  $\beta_l$  in  $M_l$ . The third parameter  $\gamma_l$  comes from an additional term  $\gamma_l u_{xx}^2$  in  $M_l$  to emphasize second-order derivatives.

A second example, is given by using the 2D PDE operator  $\mathcal{L}(u) = \Delta u + f(x, y, t)$ , with  $u|_{t=0} = 0$  and  $u|_{\partial\Omega} = 0$ . The righthand-side function is defined as  $f(x, y, t) = u_t^* - \Delta u^*$  such that the exact solution of the PDE is  $u^*(x, y, t) = (1 - e^{-t})(1 + \sin^{10}(\pi x) \sin^{10}(\pi y))$ . Figure (16) (two upper plots) shows the grids for two values of  $\alpha_l$  at steady-state ( $t = 10$ ). The two lower plots give grids for the same model but now for MFD (left) and MFE (right). Note that MFD positions its grid points near high first-order derivatives (as constructed), whereas MFE concentrates its grid at points with high second derivatives (as conjectured by (26)). Further numerical experiments should be performed to get a complete picture and to draw final conclusions on the robustness and efficiency of the deformation method.

### 3.3.2 Other Techniques

In this subsection a range of other (important) moving grid techniques will be noted. Each method is only briefly highlighted with references for more detailed information. Note that this list is far from complete. For a more extensive overview, the reader is referred to papers such as Thompson [42] and Hawken et al [23].

In Huang et al [25] the idea of so-called moving-mesh PDEs (MMPDEs) is introduced. In fact, equations (7) and (28), (32) can be derived as spe-

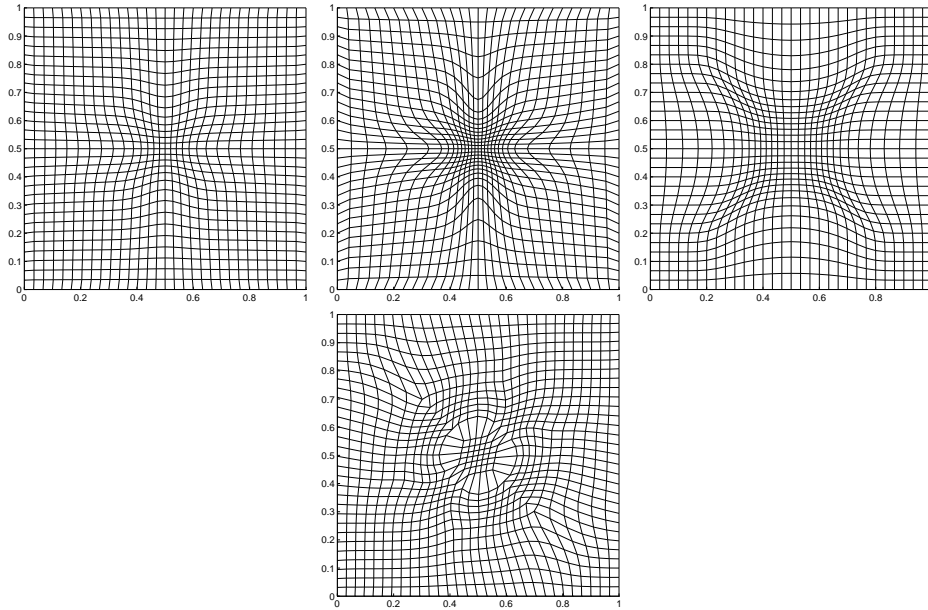


Figure 16: Moving grid results for a 2D diffusion PDE. The upper two figures show grids for the deformation method ( $\alpha_l = 2$  left and  $\alpha_l = 10$  right), the lower two figures show grids for MFD (left) and MFE (right).

cial cases of this idea. Starting from equation (7) one can create different kinds of PDEs describing the mesh movement in a continuous setting. A two-dimensional MMPDE is analyzed in Huang et al [26]. There the grid velocities  $\frac{\partial x}{\partial \theta}$  and  $\frac{\partial y}{\partial \theta}$  are derived from a heat flow equation which arises using a mesh adaptation functional that is motivated from the theory of harmonic maps. Both adaptivity and a suitable level of mesh orthogonality can be preserved.

In Arney et al [3] a moving mesh technique for hyperbolic PDE systems in two space dimensions is described. The mesh movement is based on an algebraic node movement function which is determined from the geometry and propagation of regions having significant discretization error indicators. Error clusters are moved according to the differential equation  $\ddot{\mathbf{r}} + \lambda \dot{\mathbf{r}} = 0$ , where  $\mathbf{r}$  is the position vector of the center of an error cluster. Several numerical examples are given there, among others, for the hyperbolic PDE (18) and for the Euler equations for a perfect inviscid fluid. Also an example is given where two pulses rotate in an opposite direction, indicating the need

for static rezoning, i.e.  $h$ -refinement combined with  $r$ -refinement.

In Rai et al [38] grid speed equations are given in terms of time-derivatives of the variables  $\xi$  in 1D and  $\xi$  and  $\eta$  in 2D. Their idea is to relocate the mesh points by attracting other grid points to regions where  $|u_\xi|$  is larger than its average value  $|u_\xi|_{av}$  and repelling points from regions where  $|u_\xi|$  is smaller than  $|u_\xi|_{av}$ . The attraction is attenuated by an inverse power of the point separation in the transformed domain. The collective attraction of all other points is then made to induce a velocity for each grid point. In Anderson et al [1], [2] the relation of equidistribution with Poisson grid generators, and other possible choices for the grid movement are discussed.

In Delillo et al [18] the grid is moved through an adaptation procedure that is based on a tension spring analogy, with spring constants depending on gradients in the flow of the PDE. This approach is closely related to the ideas of Brackbill et al [12], Rai et al [38] and the equidistribution principle.

One of the first moving grid methods stems from Yanenko et al [45]. They use a variational scheme which allows the grid some movement with the PDE solution and keeping control over the possible grid distortions. Their ideas are based on minimizing a functional that depends on three measures: (preventing) grid distortion, movement with the flow, and refinement whenever the gradients of the solution become large.

Another variational approach is described by Brackbill et al [12], who obtain an adaptive moving grid from the Euler equations for minimization of:  $I = \lambda_s I_s + \lambda_v I_v + \lambda_o I_o$ , where  $I_s = \int_\Omega ((\nabla\xi)^2 + (\nabla\eta)^2) d\Omega$  represents the smoothness of the grid,  $I_o = \int_\Omega (\nabla\xi \cdot \nabla\eta)^2 d\Omega$  stands for the orthogonality in the grid, and  $I_v = \int_\Omega W \mathcal{J} d\Omega$  denotes the weighted volume variation ('adaptivity'). The  $W$  and  $\mathcal{J}$  are a monitor function, and the Jacobian of the transformation, respectively. Deriving the Euler equations for this variational problem yields a system of elliptic PDEs for the grid variables. In Dietachmayer et al [19] this variational method is closely followed and applied to PDEs from meteorological models.

In Lee et al [30] an moving grid is studied that is based on equidistribution of a weight function. Their grid is smoothed by coupling neighbouring weight function values to neighbouring grid points. In the formulation, the influence of the neighbouring values of the weight function is assumed to decay exponentially with the distance from a reference grid point. Partial control over the skewness of the grid is then obtained as well.

Other interesting papers on moving-grid techniques can be found in Coyle et al [17] (on the stability of the grid selection procedure), in Kuprat [29] (on moving finite elements for surfaces), in Kansa et al [28] (application to gas dynamic equations) and Smooke et al [41] (application to chemical

reactions).

## 4 Research Issues and Summary

In this manuscript we have described several major moving grid techniques. It is clear that these techniques could be superior compared with their non-moving counterparts. As a final remark in this context Table 1 displays the results for the 2D advection model (18). Especially, note the small percentage errors of MFE and MFD for  $U_{max}$  and  $U_{min}$ , whereas FFE (‘fixed’ FE) and FFD show the well-known damping of the peak of the pulse, and oscillations behind the pulse. However, a user should always be aware of the appearance of grid distortion, whatever method is being used for the grid movement.

In one space dimension moving grid techniques are now well-established. Both MFD as (GW)MFE (and other techniques as well) have been applied to a large number of PDE models stemming from various application areas. A clear example to illustrate the difference between the residual-minimization based MFE and the equidistribution-based MFD is given in Figure 17. The PDE model belonging to this example is the advection-diffusion equation with

$$\mathcal{L}(u) = \delta \frac{\partial^2 u}{\partial x^2} - \frac{\partial u}{\partial x}, \quad (35)$$

and  $\delta = 10^{-3}$ ,  $u|_{t=0} = e^{-20x}$ ,  $u|_{x=0} = 1$ ,  $u|_{x=1} = 0$ . The solutions are oscillation-free for both moving grid methods, but the grids obey completely different criteria.

For parabolic models such as for the 2D spatial operator

$$\mathcal{L}(u) = \Delta u + \frac{e^{20}}{4}(2 - u)e^{-20/u}, \quad (36)$$

with  $u|_{t=0} = 1 + \sin^{30}(\pi x) \sin^{30}(\pi y)$  and  $u|_{\partial\Omega} = 1$ , similar equidistribution-type behaviour is observed. In Figure 18 grids for both methods are displayed for large points of time (steady-state). The difference between the two grids is mainly reflected in the positioning of the grid points near areas of high first or second-order spatial derivatives.

It must be noted that (GW)MFE and the deformation method can be formulated, in principle, in ‘any’ space dimension. The main research must therefore be focussed on efficient moving grid methods in two and three space dimensions. For (GW)MFE one must realize its connection with the method of characteristics for hyperbolic equations, and as a consequence the possibility of grid degeneration.

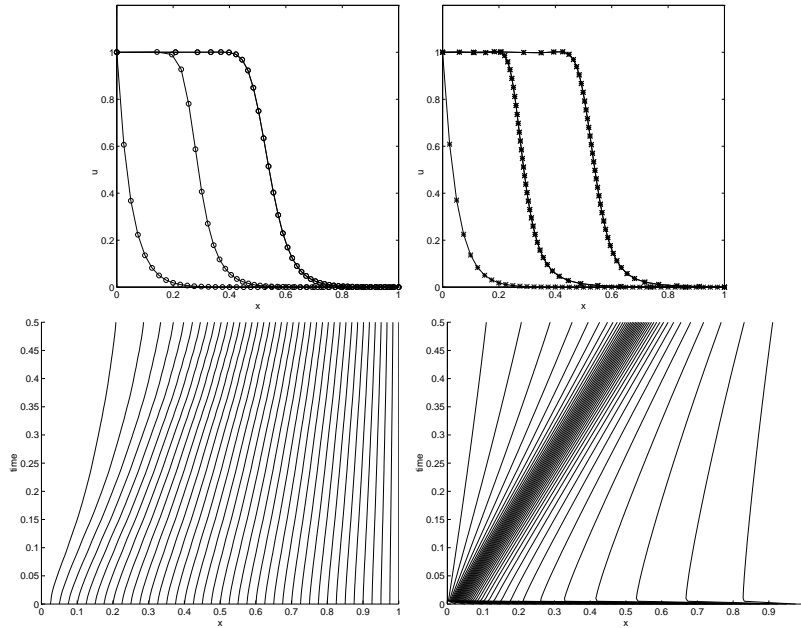


Figure 17: MFE (left) and MFD (right) results for the 1D advection-diffusion equation (35). Upper two figures show solutions on a moving grid. The lower two figures show the grid movement in time (all runs with  $\delta = 10^{-3}$ ).

The MMPDE-approach and the deformation method are relatively new techniques, that still have to be examined and tested further. Finally, for general real-life applications, a combination of  $h$ - and  $r$ -refinement (see for example Capon et al [13]) could be beneficial.

## References

- [1] D. A. Anderson. Application of adaptive grids to transient problems. In: I. Babuška, J. Chandra, J.E. Flaherty, eds., *Adaptive Computational Methods for PDEs*, SIAM, Philadelphia, 1983.
- [2] D. A. Anderson. Equidistribution schemes, Poisson generators, and adaptive grids. *Appl. Math. and Comput.*, V 24, pp. 211-227, 1987.

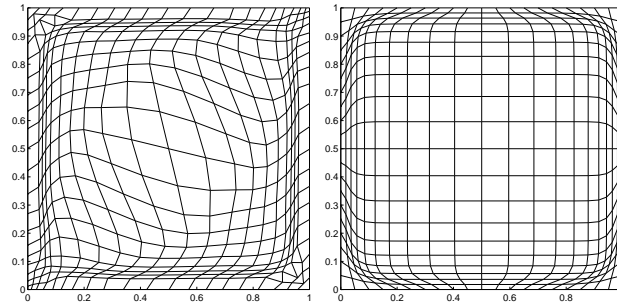


Figure 18: Steady-state grids for the 2D reaction-diffusion PDE (36); left: MFE, and right: MFD.

- [3] D. C. Arney and J. E. Flaherty. A two-dimensional mesh moving technique for time-dependent partial differential equations. *J. Comput. Phys.*, V67, pp. 124-144, 1986.
- [4] D. C. Arney and J. E. Flaherty. An adaptive local mesh refinement method for time-dependent partial differential equations. *Appl. Numer. Math.*, V5, pp. 257-274, 1989.
- [5] D. C. Arney and J. E. Flaherty. An adaptive mesh-moving and local refinement method for time-dependent partial differential equations. *Appl. Math. Comp.*, V5, pp. 257-274, 1990.
- [6] M. J. Baines. *Moving Finite Elements*. Clarendon Press, Oxford, 1994.
- [7] M. J. Baines. Properties of a grid movement algorithm. *Numerical analysis report 8/95, University of Reading, 1995*.
- [8] M. J. Berger and J. Olinger. Adaptive mesh refinement for hyperbolic partial differential equations. *J. Comput. Phys.*, V53, pp. 484-512, 1984.
- [9] J. G. Blom and P. A. Zegeling. Algorithm 731: a moving-grid interface for systems of one-dimensional time-dependent partial differential equations. *ACM Transactions in Mathematical Software*, V20, N3, pp. 194-214, 1994.
- [10] P. Bochev, G. Liao and G. de la Pena. Analysis and computation of adaptive moving grids by deformation. *Numer. Meth. for PDEs*, V12, pp. 489-506, 1996.

- [11] C. de Boor. Good approximation by splines with variable knots, II. In *Springer Lecture Notes Series 363*, Springer-Verlag, New York, 1973.
- [12] J. U. Brackbill and J. S. Saltzman. Adaptive zoning for singular problems in two dimensions. *J. Comput. Phys.*, V46, pp.342-368, 1982.
- [13] P. J. Capon and P. K. Jimack. On the adaptive finite element solution of partial differential equations using h-r-refinement. *Report 96.13, School of Computing, University of Leeds, 1996.*
- [14] N. Carlson and K. Miller. Design and application of a gradient-weighted moving finite element code I, in one dimension. *SIAM J. Sci. Comput.*, 19:728-765, 1998.
- [15] N. Carlson and K. Miller. Design and application of a gradient-weighted moving finite element code II, in two dimensions. *SIAM J. Sci. Comput.*, 19:766-798, 1998.
- [16] R. Courant and D. Hilbert. *Methods of Mathematical Physics, vol.2.* Wiley, New york, 1962.
- [17] J. M. Coyle, J. E. Flaherty, R. Ludwig. On the stability of mesh equidistribution strategies for time-dependent partial differential equations. *J. Comput. Phys.*, V62, pp. 26-39, 1986.
- [18] T. K. DeLillo and K. E. Jordan. Some experiments with a dynamic grid technique for fluid flow codes. In: R. Vichnevetsky and R. .S. Stepleman, eds., *Advances in Computer Methods for Partial Differential Equations*, IMACS, 1987.
- [19] G. S. Dietachmayer and K. K. Droegemeier. Application of continuous dynamic grid adaption techniques to meteorological modeling. Part I: basic formulation and accuracy. *Monthly Weather Review*, V120, N8, pp. 1675-1706, 1992
- [20] A. Doelman, T. J. Kaper and P. A. Zegeling. Travelling waves in the 1-d self-replicating equations. *Nonlinearity*, V10, pp. 523-563, 1997.
- [21] H. A. Dwyer, B. R. Sanders and F. Raiszadek. Ignition and flame propagation studies with adaptive numerical grids. *Combustion and Flame*, V52, pp. 11-23, 1983.
- [22] R. M. Furzeland, J. G. Verwer and P. A. Zegeling. A numerical study of three moving grid methods for one-dimensional partial differential

equations which are based on the method of lines, *J. Comput. Phys.*, V89, pp. 349-388, 1990.

- [23] D. F. Hawken, J. J. Gottlieb and J. S. Hansen. Review of some adaptive node-movement techniques in finite-element and finite-difference solutions of partial differential equations. *J. Comput. Phys.*, V95, pp. 254-302, 1991.
- [24] W. Huang and R. D. Russell. Analysis of moving mesh partial differential equations with spatial smoothing. *Research report No. 93-17*, Simon Fraser University, Burbaby, B.C., 1993.
- [25] W. Huang, Y. Ren and R. D. Russell. Moving mesh partial differential equations (MMPDEs) based on the equidistribution principle. *SIAM J. Numer. Anal.*, V31, N3, pp. 709-730, 1994.
- [26] W. Huang and R. D. Russell. Moving mesh strategy based upon a heat flow equation for two dimensional problems. *Technical report No. 96-04-03*, Dept. of Maths., University of Kansas, 1996.
- [27] W. Huang and D. M. Sloan. A simple adaptive grid method in two dimensions. *SIAM J. Sci. Comput.*, V15, N4, pp. 776-797, 1994.
- [28] E. J. Kansa, D. L. Morgan and L. K. Morris. A simplified moving finite difference scheme: application to dense gas dispersion. *SIAM J. Sci. Comput.*, V5, pp. 667-683, 1984.
- [29] A. Kuprat. Adaptive smoothing techniques for 3-D unstructured meshes. B. K. Soni, J. F. Thompson, J. Haeuser and P. Eiseman, eds. *5th International Conference on Numerical Grid Generation in Computational Computational Field Simulation*, Starkville, MSU, 1996.
- [30] D. Lee and Y. M. Tsuei. A modified adaptive grid method for recirculating flows. *Int. J. for Numer. Meth. in Fluids*, V14, pp. 775-791, 1992.
- [31] G. Liao and D. Anderson. A new approach to grid generation. *Appl. Anal.*, V44, pp. 285-298, 1992.
- [32] G. Liao and J. Su. Grid Generation via Deformation. *Appl. Math. Let.*, V5, N3, 1992.
- [33] F. Liu, S. Ji and G. Liao. An adaptive grid method and its application to steady Euler flow calculations. *SIAM J. Sci. Comput.*, 20:811-825, 1998.

- [34] K. Miller and R.N. Miller. Moving finite elements I. *SIAM J. Numer. Anal.*, 18:1019–1032, 1981.
- [35] K. Miller. Moving finite elements II. *SIAM J. Numer. Anal.*, 18:1033–1057, 1981.
- [36] L. R. Petzold. A description of DASSL: a differential/algebraic system solver. In: R. S. Stepleman, eds., *IMACS Trans. on Scientific Computation*, 1983.
- [37] L. R. Petzold. Observations on an adaptive moving grid method for one-dimensional systems of partial differential equations. *Appl. Numer. Math.*, V3, pp. 347-360, 1987.
- [38] M. M. Rai and D. A. Anderson. Grid evolution in time asymptotic problems. *J. Comput. Phys.*, V43, pp.327-344, 1981.
- [39] Y. Ren and R. D. Russell. Moving mesh techniques based upon equidistribution, and their stability. *SIAM J. Sci. Stat. Comp.*, V13, N6, pp. 1265-1286, 1992.
- [40] W. Semper and G. Liao. A moving grid finite-element method using grid deformation. *Numer. Meth. for PDEs*, V11, pp. 603-615, 1995.
- [41] M. D. Smooke and M. L. Koszykowski. Two-dimensional fully adaptive solutions of solid-solid alloying reaction. *J. Comput. Phys.*, V62, pp. 1-25, 1986.
- [42] J. F. Thompson. A survey of dynamically-adaptive grids in the numerical solution of partial differential equations. *Appl. Numer. Maths.*, V1, pp. 3-27, 1985.
- [43] R. A. Trompert and J. G. Verwer. A static-regridding method for two-dimensional parabolic partial differential equations. *Appl. Numer. Maths.*, V8, pp. 65-90, 1991.
- [44] J. G. Verwer, J. G. Blom, R. M. Furzeland and P. A. Zegeling. A moving-grid method for one-dimensional PDEs based on the method of lines. In: J. E. Flaherty, P. J. Paslow, M. S. Shephard and J. D. Vasilakis, eds., *Adaptive Methods for Partial Differential Equations*, SIAM, Philadelphia, 1989.
- [45] N. N. Yanenko, E. A. Krosenko, V. V. Liseikin, V. M. Fomin, V. P. Shapeev and Yu. A. Shitov. Methods for the construction of moving

grids for problems of fluid dynamics with big deformations. *Lecture Notes in Physics, Springer Verlag*, V59, pp. 454-459, 1976.

- [46] P. A. Zegeling. Moving-grid methods for time-dependent partial differential equations. *CWI-tract No.94*, Centre for Mathematics and Comp. Science, Amsterdam, 1993.
- [47] P. A. Zegeling, J. G. Verwer and J. C. H. v. Eijkeren. Application of a moving-grid method to a class of 1d brine transport problems in porous media. *Int. J. for Numer. Meth. in Fluids*, V15, N2, pp. 175–191, 1992.
- [48] P. A. Zegeling and J. G. Blom. A note on the grid movement induced by MFE. *Int. J. for Numer. Meth. in Eng.*, V35, N3, pp. 623–636, 1992.
- [49] P. A. Zegeling. Moving-finite-element solution of time-dependent partial differential equations in two space dimensions. *Comp. Fluid Dyn.*, V1, pp. 135–159, 1993.
- [50] P. A. Zegeling. A dynamically-moving adaptive grid method based on a smoothed equidistribution principle along coordinate lines. B. K. Soni, J. F. Thompson, J. Haeuser and P. Eiseman, eds. *5th International Conference on Numerical Grid Generation in Computational Computational Field Simulation*, Starkville, MSU, 1996.

## For Further Information

Papers on moving grid techniques are published in various journals, a.o. the "Journal of Computational Physics", "Numerical Methods for PDEs", "Applied Numerical Mathematics", "SIAM Journal on Scientific Computing", "SIAM Journal on Numerical Analysis", the "International Journal for Numerical Methods in Engineering", and the "International Journal for Numerical Methods in Fluids".

Proceedings of several conferences and workshops present a number of papers on this subject, for example, *Adaptive Methods for Partial Differential Equations*, SIAM Philadelphia, 1989 (Eds. J. E. Flaherty, P. J. Paslow, M. S. Shephard and J. D. Vasilakis), or *Grid Adaptation in Computational PDEs*, as a special issue of "Applied Numerical Mathematics", V26, N1-2, 1998.

More detailed are the works Carlson et al [14, 15] for moving finite elements, Zegeling [46] for moving finite differences, and Thompson [42], Hawken et al [23] for an overview of moving grid techniques.

Moving grid codes are available at "<http://www.cwi.nl/gollum/MOVGRD.html>" and "<http://www.math.purdue.edu/carlson/>". The former is a code (see also Blom et al [9]) for a general class of time-dependent PDEs using a moving finite difference technique based on equidistribution with smoothing in the spatial and temporal direction. The latter uses a moving finite element technique (see e.g. Carlson et al [14]) with a gradient-weighted innerproduct. More information on codes with MMPDE's can be found on <http://www.engineering.ucsb.edu/shengtai/> and then look for SFU code.